Journal of Biomedical Optics 9(6), 1122–1128 (November/December 2004)

Elastic scattering spectroscopy for intraoperative determination of sentinel lymph node status in the breast

Kristie S. Johnson
National Medical Laser Centre
University College London
Royal Free and University College Medical School
Academic Division of Surgical Specialities
and Department of Surgery
Charles Bell House
67-73 Riding House Street
London W1W 7EJ, United Kingdom

Dennis W. Chicken
National Medical Laser Centre
University College London
London, United Kingdom

David C. O. Pickard
National Medical Laser Centre
University College London
London, United Kingdom

Andrew C. Lee
Gavin Briggs
National Medical Laser Centre
University College London
London, United Kingdom

Mary Falzon
University College London
Department of Histopathology
London, United Kingdom

Irving J. Bigio
Boston University
Departments of Biomedical Engineering
and Electrical Engineering
Boston, Massachusetts

Mohammed R. Keshtgar
University College London
Royal Free and University College Medical School
Academic Division of Surgical Specilaities and
Department of Surgery
London, United Kingdom

Stephen G. Bown
National Medical Laser Centre
University College London
London, United Kingdom

Abstract. The ability to provide the best treatment for breast cancer depends on establishing whether or not the cancer has spread to the lymph nodes under the arm. Conventional assessment requires tissue removal, preparation, and expert microscopic interpretation. In this study, elastic scattering spectroscopy (ESS) is used to interrogate excised nodes with pulsed broadband illumination and collection of the backscattered light. Multiple spectra are taken from 139 excised nodes (53 containing cancer) in 68 patients, and spectral analysis is performed using a combination of principal component analysis and linear discriminant analysis to correlate the spectra with conventional histology. The data are divided into training and test sets. In test sets containing spectra from only normal nodes and nodes with complete replacement by cancer, ESS detects the spectra from cancerous nodes with 84% sensitivity and 91% specificity (per-spectrum analysis). In test sets that included normal nodes and nodes with partial as well as complete replacement by cancer, ESS detects the nodes with cancer with an average sensitivity of 75% and specificity of 89% (per-node analysis). These results are comparable to those from conventional touch imprint cytology and frozen section histology, but do not require an expert pathologist for interpretation. With automation of the technique, results could be made available almost instantaneously. ESS is a promising technique for the rapid, accurate, and straightforward detection of metastases in excised sentinel lymph nodes. [DOI: 10.1117/1.1802191]

Keywords: elastic scattering spectroscopy; lymph node staging; breast cancer; diagnostic optical spectroscopy; optical biopsy; sentinel node.

Paper 94002 received Dec. 3, 2003; revised manuscript received Mar. 19, 2004; accepted for publication Mar. 19, 2004.

1 Introduction

Breast cancer is the most common malignancy in women in the western world, with a reported incidence of up to 1 in 8 women. The presence or absence of metastatic cancer in the axillary lymph nodes in patients with breast cancer remains the most powerful predictor of prognosis, and plays an important role in identifying patients who are at risk of developing disease that spreads throughout the body, who are likely to benefit from chemotherapy. Traditionally, the presence of axillary lymph node metastases has been determined by axillary lymph node dissection (ALND), which is a surgical procedure that removes all the lymph nodes under the arm. This is a substantial surgical procedure, however, which can be associated with several serious side effects, the most significant being lymphoedema (persistent swelling of the arm) and shoulder dysfunction, which adversely affect the patient's quality of life.[1]

In current surgical practice, most patients present with early disease as a result of increased public awareness of breast cancer and mammography screening programs. Hence most patients do not have axillary lymph node metastases at presentation, and while the staging information is crucial for their future management, they get no therapeutic benefit from ALND, while still being at risk of developing the complications associated with the procedure.

Address all correspondence to Professor Stephen Bown, National Medical Laser Centre, University College London, Charles Bell House, 67-73 Riding House Street, London W1W 7EJ, U.K. Tel: 44(0)2076799060; Fax: 44(0)2078132828; E-mail: s.bown@ucl.ac.uk

The sentinel node is any lymph node with a direct lymphatic connection to the tumor, and by definition is the first node to be invaded by cancer spreading from the breast. It has been well documented that if cancer cannot be detected in sentinel nodes, the chance of there being any cancer in nodes further down the chain draining the breast is exceedingly small.[2] Thus if the sentinel node can be easily identified, removed, and examined for cancer and no cancer is found, there is no need to remove the rest of the axillary nodes. This markedly reduces the risk of complications associated with full axillary node clearance.[3,4]

To get the maximum benefit from sentinel node biopsy, it is important to be able to determine rapidly whether or not cancer is present. If the assessment cannot be completed while the patient is still on the operating table, the subsequent discovery of cancer in the node will necessitate a second operation to perform the ALND. This gives rise to additional costs and causes further anxiety to the patient.

Traditionally, intraoperative diagnosis of sentinel nodes has been done by histological examination of frozen sections. In practice, because of their soft texture, frozen sections of lymph nodes are technically difficult to prepare and interpretation may be difficult. Accurate results from frozen sections rely on the skill of an experienced pathologist. It is therefore not surprising that there is wide variation in the reported accuracy of this technique. The best results are those reported by the European Institute of Oncology in Milan, but these were only achieved by 50-μm sectioning. Exhaustive frozen section examination is highly accurate (sensitivity=93.7%),[5] but consumes vast resources and is time consuming, and therefore is not appropriate in the setting of smaller hospitals. Routine frozen section examination of sentinel nodes has yielded more disappointing results, with sensitivities ranging from 44 to 87%.[6,7]

Touch imprint cytology (direct imprinting of the tissue onto a thin glass slide, staining the cells, and examining them under a microscope) is one of the oldest techniques in cytology and is now being applied to the examination of sentinel lymph nodes. It is quick and easy to perform and gives similar results to frozen sections.[7–10] Both techniques, however, are reliant on the availability of a highly skilled cytopathologist, and it is likely that the excellent results reported from specialist units will not be replicated in smaller hospitals relying on a general pathologist for reporting.

The lack of a more generally available and reliable intraoperative tool to establish the sentinel node status remains an obstacle to the routine practice of sentinel node biopsy. A real-time optical method for determining sentinel node involvement would provide significant benefits to patients undergoing surgery for breast cancer. Elastic scattering spectroscopy (ESS), when performed using an appropriate optical geometry[11,12] (as shown in Fig. 1) is sensitive to the sizes, indices of refraction, and structures of the subcellular components (e.g., nucleus, nucleolus, and mitochondria) that change with malignant transformation.[13] The measured ESS spectra relate to the wavelength dependence and angular probability of the scattering efficiency of tissue microcomponents, as well as to absorption bands. Consequently, based on the fact that many tissue pathologies and most cancers exhibit morphological changes at the cellular and subcellular level, this approach generates spectral signatures that reflect the changing tissue parameters that pathologists address. These include the size and shape of nuclei and organelles, the nucleocytoplasmic ratio, and chromatin density. Both Mie theory[11,12] and finite-difference time domain methods[14] have been employed successfully to model spectral changes resulting from malignant transformation. Multivariate statistical analysis can be used to recognize patterns within the spectra, which can then be used to discriminate between spectra from malignant and benign tissue once appropriate diagnostic algorithms have been developed.

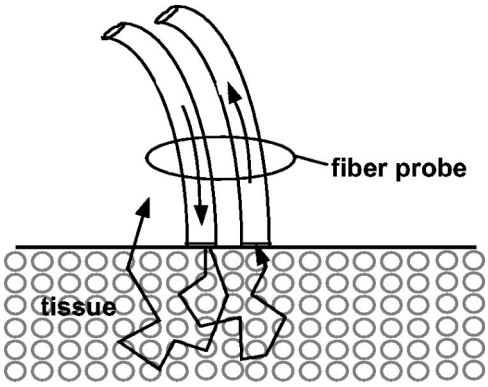

Fig. 1 Depiction of the optical probe geometry used in the ESS method. The fiber tips are in optical contact with the tissue surface. With a fiber separation of ≤ 350 μm (center to center), only light that has scattered elastically a small number of times and at a large angle within a shallow layer is collected.

Analysis of ESS spectra has the potential to provide an instant diagnosis for use during surgery, which would be ideal for differentiating sentinel nodes with and without cancer. Further, the results are not subjective and do not require interpretation by a pathologist. ESS has been studied previously as a minimally invasive diagnostic technique where access to the tissue is achieved using either direct topical access or mediated by endoscopy.[15–17] We have previously reported the results of a pilot study on the use of ESS in the assessment of breast tissue and axillary nodes.[18]

We present the results of the second phase of our study on sentinel node assessment in breast cancer using elastic scattering spectroscopy, in which a larger dataset and new statistical methods have been used.

2 Materials and Methods

2.1 *Elastic Scattering Spectroscopy System*

The ESS instrumentation consists of a pulsed xenon arc lamp, an optical probe, a spectrometer, and a computer to control the various components and record the spectra. The arc lamp, spectrometer, and power supply are housed in a briefcase-size unit to which the laptop computer is connected. ESS involves directing short pulses (~ 1 μs) of white light (320 to 920 nm) from the pulsed xenon arc lamp (Perkin Elmer, Incorporated) through a flexible optical fiber (400 μm) touching the tissue to be interrogated. Ultraviolet B (280 to 315 nm) and ultraviolet C (100 to 280 nm) light is filtered out to avoid any potential risk to patients. A collection fiber (200 μm), with a fixed separation distance of ~ 350 μm from the first fiber (center-to-center), collects light scattered from the upper layers of the

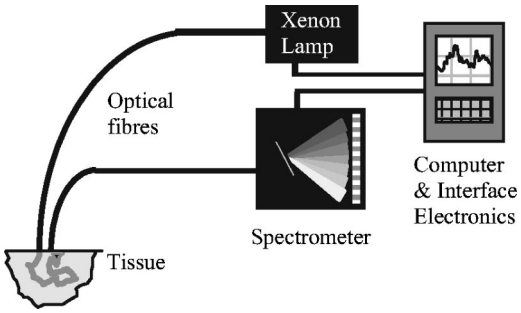

Fig. 2 Schematic diagram of elastic scattering spectroscopy (ESS) system.

tissue and propagates it to the spectrometer (S2000 Ocean Optics), which outputs the spectrum to the laptop computer for recording and further analysis.

Figure 2 shows a schematic diagram of the system. The whole fiber assembly measures 1.5 mm in diameter and the distal end is housed in a rigid stainless steel casing for easy handling and sterilization. The collection and recording of a single spectrum takes less than a quarter of a second, with the integration time of the detector (20 to 40 ms per pulse) being the limiting factor.

Before any spectra of the lymph nodes are taken, a white reference spectrum is recorded. This establishes the system response by recording the diffuse reflectance from a flat surface of Spectralon™ (Labsphere, Incorporated), which is spectrally flat between 250 and 1000 nm. The reference spectrum allows spectral variations in the light source, spectrometer, fiber transmission, and fiber coupling to be accounted for. Each consequent lymph node spectrum was divided by this spectrum to give the system-independent spectrum of the site being investigated. Immediately prior to (100 ms before) any spectral measurement (Spectralon or tissue), the automated system records a ''dark'' spectrum (without triggering the lamp), which is subtracted from the spectrum (with lamp) that follows. Thus, the tissue spectrum that is stored and displayed is determined by the expression: $S_{\text{tissue}}-D_{\text{tissue}}/S_{\text{ref}}-D_{\text{ref}}$, where ref indicates a measurement with the Spectralon reference material, S indicates a spectrum recording with the lamp triggered and D indicates a dark recording without the lamp. In this manner, the site-specific ambient light at the moment of measurement and the detector dark current are accounted for.

2.2 *Clinical Acquisition of Elastic Scattering Spectra*

This study was approved by the ethics committee (Institutional Review Board) of the University College London Hospitals and informed consent was obtained, prior to their participation, from patients with breast cancer undergoing either sentinel node biopsy or axillary node clearance. Sentinel nodes were identified using the combination technique of preoperative sentinel node imaging using Tc^{99}-labeled albumin colloid with intraoperative gamma probe guided detection and blue dye injection.[19] All removed nodes were bivalved, and spectra were taken from the cut surfaces of both halves. The tip of the optical probe was held perpendicular to the cut surface in gentle contact with the tissue, and the lamp and spectrometer were triggered using either a foot pedal or via the laptop keyboard. Between 2 and 20 spectra were collected per node (depending on the size of the node) with measurements from various locations, including subcapsular and central regions of the node.

2.3 *Histopathology*

After the spectra had been taken, the bivalved lymph nodes were fixed in formalin and sent for histopathological processing. For sentinel nodes, this consisted of routine three level paraffin-embedded sections, with the addition of immunohistochemistry (IHC) for cytokeratin if the hematoxylin and eosin (H and E) staining did not show any tumor. Nonsentinel nodes (bivalved) were sectioned through a single level and stained only with H and E.

It was not possible to obtain the histological diagnosis specific to the site (within the node) of each spectral measurement, as this would involve microdissection of the nodes that could interfere with the overall histological analysis. To reduce the effect of this lack of one-to-one correlation, the lymph nodes were classified as either normal or metastatic, and the metastatic nodes were subdivided into those nodes with total replacement by cancer, partial replacement by cancer, minute areas (<2 mm in diameter) of replacement by cancer (micrometastases), and those which showed cancer detectable only using IHC.

2.4 *Spectral Processing*

All the spectra used in the analysis underwent smoothing, in which each intensity point was replaced by the average of the 20 neighboring intensity points (namely, moving average smoothing with a span of 20 points). The smoothed data were then reduced from the 1801 points, corresponding to the spectrometer resolution, down to 180 intensity values, to speed further manipulation. The wavelength window used was reduced from 320 to 920 nm to $\sim$340 to 900 nm, to remove the regions of the spectra with low signal-to-noise ratios arising from the lower light intensity emitted by the Xenon arc lamp at the extremes of its output spectrum.

Each smoothed spectrum was then standardized by subtracting the mean intensity of the spectrum (i.e., the average intensity over the full spectral range) from each data point. Each point was then divided by the standard deviation of the smoothed spectrum. This method of standardization gave all the spectra a mean intensity of zero and a standard deviation equal to one. Using this standardization meant that only the relative intensities across the whole wavelength range were important and not the actual light intensity, and as such the number of light pulses used to generate a spectrum did not have to be taken into account when analyzing the spectra. In the set of spectra used in this analysis, no obvious outliers were detected; however, a number of spectra (unstandardized) were found to be negatively saturated (i.e., intensity of zero) at $\sim$420 or $\sim$550 nm, corresponding to the hemoglobin absorption peaks. In all cases the spectra were saturated only at the center of the peaks and not anywhere else. This saturation was considered to have a minimal effect on the rest of the spectrum, so these spectra were not removed from the analysis.

Principal component analysis (PCA) was applied to the spectra to reduce the data to only those regions with large

Table 1 Distribution of the histological classification of the axillary lymph nodes used in this study.

	Nodes	Spectra
Total number in study	139	782
Normal nodes	86	394
Metastatic nodes		
Total metastases	25	219
Partial metastases	22	114
Micro-metastases and metastases only positive on IHC	6	55
Total number of metastatic nodes	53	388

variability. This was carried out using the statistical package Systat. Linear discriminant analysis (LDA) was then carried out (also using Systat) on the principal components to improve on the discrimination between the normal and metastatic nodes.

3 Results

A total of 139 (sentinel and nonsentinel axillary nodes) from 68 patients were used in this study. Of these, 53 were shown to contain cancer on histology (metastatic nodes) and in 86, no cancer could be detected (normal nodes). Details are summarized in Table 1. From the spectra, 20 principal components were extracted, to include any spectral component contributing more than 0.01% of the variability. A plot of the first two principal components, shown in Fig. 3, immediately showed some obvious discrimination between metastatic and normal nodes.

Linear discriminant analysis (LDA) was subsequently carried out (also using Systat) on all the principal components to improve on the discrimination between normal and metastatic nodes already shown by the first two principal components. Two different analyses were undertaken on this data; a per-spectrum analysis and a per-node analysis.

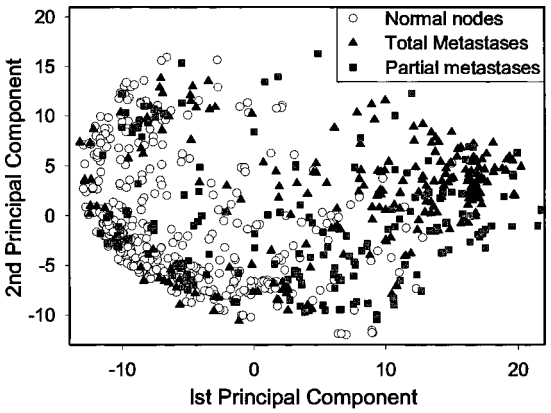

Fig. 3 Scatter plot of the first and second principal components of the ESS spectra.

In the per-spectrum analysis, only the spectra from the totally metastatic and the normal nodes were used. The partial, micro- and IHC-only metastatic nodes were excluded from this analysis due to the uncertainty of the per-spectrum histological diagnosis in these nodes. To assess the accuracy of the LDA analysis on a per-spectrum basis, a leave-one-out cross-validation was undertaken.

In general, more than one spectrum was taken per node. Thus to assess each node as a single entity, based on the combined diagnosis of all the spectra from a single node, the per-node analysis method was undertaken. In this per-node analysis, if any one of the spectra from a particular node was classified as metastatic by the LDA algorithm, the whole node was regarded as metastatic. All the nodes were used in the per-node analysis, including the partial-, micro-, and IHC metastatic nodes. The leave-one-out cross-validation in Systat was regarded as inappropriate for the per-node analysis, as Systat does not output the cross-validated diagnosis predictions for each spectrum, but rather the unvalidated diagnosis predictions. To overcome this limitation for the per-node analysis, three randomly assigned combinations of training set and test set were used for cross-validation instead of the leave-one-out method. The reason multiple training-set/test-set combinations were used as opposed to just one was to ensure that the results obtained were not training-set specific. Further, all the spectra from a particular node were allocated to either the training set or the testing set, such that systematic effects were removed. Such systematic effects are a common problem in this sort of analysis, though this is rarely recognized.

As histology was only available on a per-node basis, only the normal nodes and those with total metastatic replacement were used in the training sets for both the per-node and per-spectrum analyses. The data were split between the training and test sets, using a random number generator in Excel, such that 50% of the normal nodes and 50% of the nodes with total metastatic replacement were in the training set, and the remaining 50% of these nodes, along with the partially metastatic, micro-metastatic, and IHC nodes, were in the test set.

Patent blue dye was used to locate the sentinel nodes for excision, and as such the spectra from these nodes showed an absorption peak at $\sim$650 nm, which was not present in the nonsentinel nodes. The presence of blue dye in only the sentinel nodes was not expected to influence the analysis, since the proportion of positive and negative nodes was similar in the sentinel and nonsentinel nodes. This was confirmed in a separate analysis (data not shown).

Figure 4 shows the density of the canonical scores from the LDA for both the metastatic and normal nodes. The discrimination shown in this figure is encouraging. Only a small number of spectra from normal nodes have scores that fall into the range associated with metastatic nodes, taking the dividing diagnostic canonical score as zero. The number of spectra from metastatic nodes having scores that fall into the range associated with normal nodes was much higher, but this was expected due to the high probability of interrogating normal sites in the partially metastatic, micro-metastatic, and IHC positive nodes. As would be expected, the discrimination demonstrated in the per-node analysis scores is much better than for the per-spectrum scores.

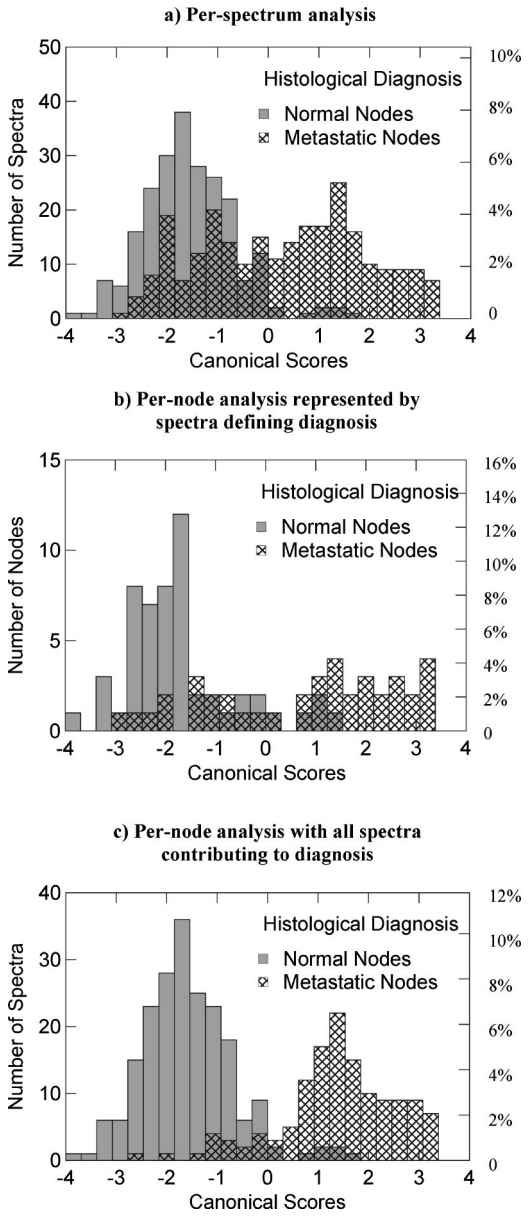

Fig. 4 Linear discriminant analysis (LDA) canonical scores for the spectra from the lymph nodes in test set 1 are shown: (a) shows the per-spectrum analysis and (b) the per-node analysis. For (b), if any one of the spectra from a particular node was classified as metastatic by the LDA algorithm, the entire node was diagnosed as metastatic. In this per-node histogram, the canonical scores shown are those of the defining spectrum (i.e., the spectrum with the most positive or negative canonical score). If all the spectra contributing to the per-node diagnosis are included, histogram (c) is achieved.

Table 2 shows a summary of the results obtained from the LDA. The per-spectrum sensitivity was 84% and the specificity was 91%. Note that the partial- and micro-metastatic nodes and IHC positive nodes were not included in this per-spectrum analysis, as mentioned earlier. The per-node analysis on all the nodes, in which one positive spectrum was taken to imply the whole node as metastatic, gave an average sensitivity of 75% and a specificity of 89%.

A breakdown of the ESS diagnoses of the metastatic nodes for the three different training-set/test-set combinations is shown in Table 3. This demonstrates the high accuracy ($\geqslant$90%) with which ESS spectra pick up the totally metastatic nodes. The detection of partial metastases was less consistent with accuracies ranging between 19 and 86%. It was interesting to find that in two of the three-training-set/test-set combinations, those nodes with micro-metastases and those positive only on IHC were detected with 100% accuracy. This may suggest some changes are occurring in the nodes in the early stages of metastasis that are not readily visible under a microscope, but which can be detected by ESS. Further work is currently underway to ascertain whether this is purely a chance occurrence or whether this is a more fundamental observation that might be exploited in future studies.

Table 2 Summary of the per-spectrum and per-node ESS diagnostic accuracy. The per-spectrum analysis was applied only to the totally metastatic and normal nodes, and the leave-one-out cross-validation method was used. The per-node analysis was applied to all the nodes and three training-set/test-set combinations were used for validation.

		Per node analysis	
	Per-spectrum analysis	Average	Range
Sensitivity (=TP/TP+FN)	84%	75%	60 to 84%
Specificity (=TN/TN+FP)	91%	89%	82 to 97%

4 Discussion

This study shows that ESS is an effective way to detect cancer in excised axillary lymph nodes. The average sensitivity per node for detecting cancer is 75% with an average specificity of 89%. One test set gave a low figure for sensitivity in nodes with only partial replacement with cancer, but this may have been related to the limited number of spectra taken from some nodes. ESS is a point measurement, and to obtain the best results from this technique, it will be necessary to develop ways of interrogating nodes more thoroughly. This can be achieved by either the collection of multiple spectra by scanning across each cut surface of the node, or by increasing the number of surfaces to be interrogated by cutting the node into multiple layers. Of course, the same sort of sampling problem applies to histo- and cyto-pathological techniques for detect-

Table 3 ESS diagnostic sensitivity for the detection of cancer for each randomly selected training/test set combination, showing the individual sensitivities for the total, partial, and micro-/IHC metastases in the test set.

	Test set 1 sensitivity	Test set 2 sensitivity	Test set 3 sensitivity
Total metastases	90%	100%	90%
Partial metastases	86%	68%	19%
Micro-metastases and IHC metastases only	60%	100%	100%

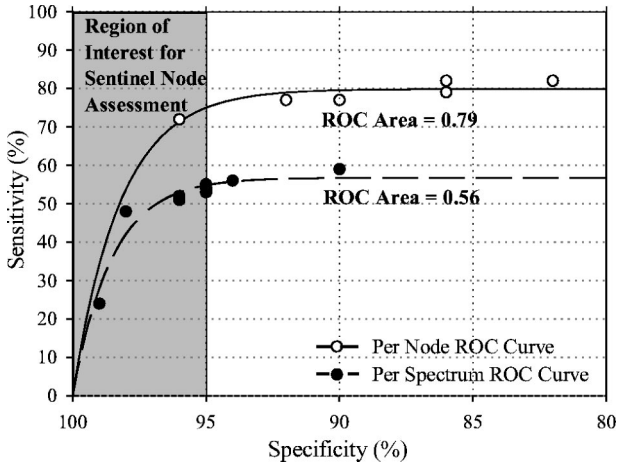

Fig. 5 ROC plot of the test set 1 LDA results for both the per-spectrum and per-node analyses, applied to all the nodes. The test set 1 sensitivity and specificity values used to calculate the averaged results given in Table 2 were those with the best overall accuracy (highest number of correct diagnoses, metastatic plus nonmetastatic) for test set 1, namely sensitivity=55% and specificity=95% for the per-spectrum analysis, and sensitivity=82% and specificity=86% for the per-node analysis.

ing cancer in nodes, (paraffin-embedded sections, frozen sections, and touch imprint cytology). None of these techniques can give 100% sensitivity, but there is little doubt that the harder one looks, the more cancer can be found in nodes. Cancer will only be detected if it is present on the cut surface of the node that is being examined. Currently, nodes examined using touch imprint cytology and ESS are limited to having only two cut surfaces, due to the practical difficulties encountered in the cutting of fresh (unfixed) nodes. Examination of multiple sections of each node may well lead to an improvement in the sensitivity in both touch imprint cytology and ESS, but before multiple sectioning can be achieved, the difficulties in cutting fresh nodes will have to be overcome. However, ESS does have the advantage over imprint cytology in that it can interrogate the tissue 0.5 to 1 mm below the surface, but it has the disadvantage that multiple spectra must be taken to fully examine a cut surface. Imprint cytology and frozen section look at the information from an entire cut surface under one microscope slide, but do not give any information from below the surface.

In expert hands, 100% specificity is achievable with frozen sections and touch imprint cytology, as both rely on positive identification of cancer cells.[7] This is important for surgeons, as no surgeon wants to undertake an unnecessary full axillary dissection as a result of a false positive diagnosis of metastatic disease. The 89% specificity of ESS cannot yet match this. Nevertheless, the ESS analysis is statistical and the figures for sensitivity and specificity have been based on taking the dividing line in Fig. 4 at a score of zero. The specificity can be increased (at the cost of reducing the sensitivity) by increasing the score defining the cut-off between normal and metastatic lymph nodes. This is shown in the receiver operating characteristic (ROC) graph shown in Fig. 5. For instance, to increase the specificity to 98%, the sensitivity would fall to 49%. Naturally ESS has the enormous advantage that it does not require an expert to interpret the findings, so the best results can be achieved by individuals with minimal training, in the absence of an expert pathologist.

In our hospital breast unit, touch imprint cytology is currently the most practical method used in sentinel node assessment, as it gives results in a matter of tens of minutes with a sensitivity of 75% and a specificity of 99%, although it does require the presence of an experienced cytologist.[20] Once the discriminating algorithm has been perfected, ESS will take only a few seconds to acquire and analyze each spectrum from an excised and sectioned lymph node.

Sentinel node biopsy is being used routinely in the staging of a range of potentially life-threatening cancers, including malignant melanoma of the skin, head and neck cancers, penile carcinoma, and vulval carcinoma. It is likely that further applications of ESS will be developed in these areas in the future[21]

At present, the analysis of ESS spectra is empirical, as it is not known which histological and cytological features are reflected in spectral changes. Studies are underway to elucidate these problems, and it is hoped that a better understanding of how spectral changes are generated will lead to the development of more accurate diagnostic algorithms. Nevertheless, the evidence we have at present suggests that ESS could become a straightforward and valuable technique for the rapid and accurate detection of metastatic breast cancer in sentinel lymph nodes.

References

1. M.W. Kissin, R.G. Querci della, D. Easton, and G. Westbury, ''Risk of lymphoedema following the treatment of breast cancer,'' *Br. J. Surg.* **73**(7), 580–584 (1986).
2. R.R. Turner, D.W. Ollila, D.L. Krasne, and A.E. Giuliano, ''Histopathologic validation of the sentinel lymph node hypothesis for breast carcinoma,'' *Ann. Surg.* **226**(3), 271–276 (1997).
3. U. Veronesi, G. Paganelli, G. Viale, A. Luini, S. Zurrida, V. Galimberti, M. Intra, P. Veronesi, C. Robertson, P. Maisonneuve, G. Renne, C. De Cicco, F. De Lucia, and R. Gennari, ''A randomized comparison of sentinel-node biopsy with routine axillary dissection in breast cancer,'' *N. Engl. J. Med.* **349**(6), 546–553 (2003).
4. K.K. Swenson, M.J. Nissen, C. Ceronsky, L. Swenson, M.W. Lee, and T.M. Tuttle, ''Comparison of side effects between sentinel lymph node and axillary lymph node dissection for breast cancer,'' *Ann. Surg. Oncol.* **9**(8), 745–753 (2002).
5. U. Veronesi, S. Zurrida, G. Mazzarol, and G. Viale, ''Extensive frozen section examination of axillary sentinel nodes to determine selective axillary dissection,'' *World J. Surg.* **25**(6), 806–808 (2001).
6. S.A. Gulec, J. Su, J.P. O'Leary, and A. Stolier, ''Clinical utility of frozen section in sentinel node biopsy in breast cancer,'' *Am. Surg.* **67**(6), 529–532 (2001).
7. P.J. Van Diest, H. Torrenga, P.J. Borgstein, R. Pijpers, R.P. Bleichrodt, F.D. Rahusen, and S. Meijer, ''Reliability of intraoperative frozen section and imprint cytological investigation of sentinel lymph nodes in breast cancer,'' *Histopathology* **35**(1), 14–18 (1999).
8. K. Motomura, H. Inaji, Y. Komoike, T. Kasugai, S. Nagumo, S. Noguchi, and H. Koyama, ''Intraoperative sentinel lymph node examination by imprint cytology and frozen sectioning during breast surgery,'' *Br. J. Surg.* **87**(5), 597-601 (2000).
9. A.J. Creager, K.R. Geisinger, S.A. Shiver, N.D. Perrier, P. Shen, S.J. Ann, P.R. Young, and E.A. Levine, ''Intraoperative evaluation of sentinel lymph nodes for metastatic breast carcinoma by imprint cytology,'' *Mod. Pathol.* **15**(11), 1140–1147 (2002).
10. A.A. Salem, A.G. Douglas-Jones, H.M. Sweetland, R.G. Newcombe, and R.E. Mansel, ''Evaluation of axillary lymph nodes using touch imprint cytology and immunohistochemistry,'' *Br. J. Surg.* **89**(11), 1386–1389 (2002).
11. J.R. Mourant, J. Boyer, A.H. Hielscher, and I.J. Bigio, ''Influence of the scattering phase function on light transport measurements in tur-

bid media performed with small source-detector separations,'' *Opt. Lett.* **21**(7), 546–548 (1996).
12. L.T. Perelman, V. Backman, M. Wallace, G. Zonios, R. Manoharan, A. Nusrat, S. Shields, M. Seiler, C. Lima, T. Hamano, I. Itzkan, J. Van Dam, J.M. Crawford, and M.S. Feld, ''Observation of periodic fine structure in reflectance from biological tissue: A new technique for measuring nuclear size distribution,'' *Phys. Rev. Lett.* **80**(3), 627–630 (1998).
13. J.R. Mourant, A.H. Hielscher, A.A. Eick, T.M. Johnson, and J.P. Freyer, ''Evidence of intrinsic differences in the light scattering properties of tumorigenic and nontumorigenic cells,'' *Cancer Cytopathol.* **84**(6), 366–374 (1998).
14. D. Arifler, M. Guillaud, A. Carraro, A. Malpica, M. Follen, and R. Richards-Kortum, ''Light scattering from normal and dysplastic cervical cells at different epithelial depths: finite-difference time-domain modeling with a perfectly matched layer boundary condition,'' *J. Biomed. Opt.* **8**(3), 484–494 (2003).
15. Z.F. Ge, K.T. Schomacker, and N.S. Nishioka, ''Identification of colonic dysplasia and neoplasia by diffuse reflectance spectroscopy and pattern recognition techniques,'' *Appl. Spectrosc.* **52**(6), 833–839 (1998).
16. J. R. Mourant, I. J. Bigio, J. D. Boyer, T. M. Johnson, J. Lacey, A. G. Bohorfoush III, and M. H. Mellow, ''Elastic scattering spectroscopy as a diagnostic tool for differentiating pathologies in the gastrointestinal tract: preliminary testing,'' *J. Biomed. Opt.* **1**(2), 192–199 (1996).
17. J.R. Mourant, I.J. Bigio, J. Boyer, R.L. Conn, T. Johnson, and T. Shimada, ''Spectroscopic diagnosis of bladder cancer with elastic light scattering,'' *Lasers Surg. Med.* **17**(4), 350–357 (1995).
18. I.J. Bigio, S.G. Bown, G. Briggs, C. Kelley, S. Lakhani, D. Pickard, P.M. Ripley, I.G. Rose, and C. Saunders, ''Diagnosis of breast cancer using elastic-scattering spectroscopy: preliminary clinical results,'' *J. Biomed. Opt.* **5**(2), 221–228 (2000).
19. H.S. Cody, J. Fey, T. Akhurst, M. Fazzari, M. Mazumdar, H. Yeung, S.D.J. Yeh, and P.I. Borgen, ''Complementarity of blue dye and isotope in sentinel node localization for breast cancer: Univariate and multivariate analysis of 966 procedures,'' *Ann. Surg. Oncol.* **8**(1), 13–19 (2001).
20. A.C. Lee, D.W. Chicken, C.D.O. Pickard, G.M. Briggs, G. Kocjan, M. Falzon, I. Bigio, P.J. Ell, J.R. Sainsbury, M.R.S. Keshtgar, and S.G. Bown, ''Comparative study of elastic scattering spectroscopy and touch imprint cytology in assessing sentinel lymph node status in breast cancer,'' *Br. J. Surg.* **90**, 112 (2003).
21. L. Maffioli, E. Sturm, M. Roselli, R. Fontanelli, E. Pauwels, and E. Bombardieri, ''State of the art of sentinel node biopsy in oncology,'' *Tumori* **86**(4), 263–272 (2000).